

Roll manufacturing of flexible microfluidic devices in thin PMMA and COC foils by embossing and lamination

Khaled Metwally · Laurent Robert ·
Samuel Queste · Bernard Gauthier-Manuel ·
Chantal Khan-Malek

Received: 3 April 2011 / Accepted: 21 September 2011 / Published online: 8 October 2011
© Springer-Verlag 2011

Abstract Microfluidics on foil is gaining momentum due to a number of advantages of employing thin films combined with the capability of cost-effective high-volume manufacturing of devices. In this work, ultra-thin, flexible Y-microreactors with microchannels of 100 μm width and 30 μm depth were fabricated in thermoplastic polymer foils. The fluidic pattern was hot roll embossed in 125 μm thick poly-methyl-methacrylate (PMMA) and 130 μm thick cyclic-olefin-copolymer (COC) films using a dry-etched microstructured silicon wafer as a flat embossing tool in a laminator. The sealing of the channels was performed with two different techniques, one based on lamination of SU8 dry film resist (DFR) and the other one based on spin-coated poly-dimethylsiloxane (PDMS). Testing of the interconnected microreactor was carried out using two dye colorant solutions to demonstrate mixing.

1 Introduction

In addition to miniaturization requirements, the need of disposability for many microfluidic components or systems, has lead to usage of polymers which are low cost and amenable to high volume manufacturing (Fiorini and Chiu 2005). Poly-methyl-methacrylate (PMMA) is an important

amorphous thermoplastic polymer for industrial and technical applications at the micro and nanoscale, where for example its superior optical transparency in the visible range, its relatively low hydrophobicity and biocompatibility are exploited in optical or/and fluidic devices. Cyclic olefin copolymer (COC) is another thermoplastic material which has recently gained attention in fabrication of microfluidic devices applications based on its various advantages with regards to physical and chemical properties. COC is highly resistant to polar solvents, acids and bases, it has a high water vapor barrier, a high optical transmission in the near-UV and visible range, a refractive index of 1.53, and it is biocompatible (Nunes et al. 2010). SU8 is the most popular negative type photoresist in microsystem technology (Abgrall et al. 2006), known in particular for its high transmission in the ultra-violet (UV) range, allowing for the production of microstructures with very high aspect ratio. It is an epoxy-based resist optimized for near UV (I line @365 nm). It has good qualities for a structural material, is mechanically strong when cross-linked. It has excellent characteristics for optical applications, with high transmittance for light from visible (above 350 nm) to near- IR range and a high refractive index (of 1.8) after hard-baking. It is also chemically stable and compatible with most chemicals (solvents, acids, bases). It is usually used in liquid form of different viscosities leading to a large range of thickness but also exists in dry film form.

Nowadays, the technology trends are going towards the usage of flexible systems in different fields, as in organic electronics and photovoltaic and most recently in sensorics, with applications such as thin film transistor (TFT) (Garnier et al. 1994), organic light emitting displays (OLEDs) (Sarma et al. 2006), radio frequency identifications (RFIDs) (Nambiar 2009), organic solar cells (OSCs) (Wohrle and Meissner 1991) and thin film batteries (TFBs)

K. Metwally is Erasmus Mundus student–European Union Master for Mechatronics and Micro-Mechatronics.

K. Metwally · L. Robert · S. Queste · B. Gauthier-Manuel ·
C. Khan-Malek (✉)
FEMTO-ST Institute, UMR CNRS 6174, 32 Avenue de
l'Observatoire, 25044 Besançon Cedex, France
e-mail: chantal.khanmalek@femto-st.fr

K. Metwally
e-mail: khaled.metwally@femto-st.fr

(Nystrom et al. 2009). There is also an increasing interest in developing microfluidics and Lab-on-a-Chip solutions based on thin films or foils (Microfluidics on a foil/Lab-on-a-Foil) (Focke et al. 2010). The realization of lab-on chip with thin film technologies open the door for different applications, particularly those requiring better heat transfer efficiency, mechanical flexibility and lower material consumption. For example they could be embedded into a wide range of innovative products such as smart cards, displays, implantable medical devices, and advanced textiles where their deformability or conformability could be exploited. Specific high-volume, price-sensitive market segments of relevance here concern low-cost, single-use disposable devices in health care industry for applications; such as point-of-care diagnostics and smart bandages, as well as in food industry for smart packaging.

Different flexible film materials such as paper, metals and polymers have been used in the fabrication of these devices. However, polymer foils can offer a lot of advantages like transparency variation, biological compatibility, full flexibility and robustness. The techniques of interest for the manufacture of polymer-foil based microfluidic devices (Focke et al. 2010) are those allowing the production of a large number of devices using for example photolithographic methods (Tsai et al. 2006; Khan-Malek and Robert 2008), lamination (Abgrall et al. 2008; Khan-Malek et al. 2009), or using replication techniques, where a master structure is replicated into the polymer material by techniques such as thermoforming (Focke et al. 2009) or embossing (Paul et al. 2007; Velten et al. 2008). Each of these manufacturing methods has its applicability, flexibility, up-scalability, robustness, and cost-efficiency. In particular, continuous processing of flexible devices using thin films can be carried via roll-to-roll manufacturing (Velten et al. 2008). Roll embossing where rollers are used instead of the plates of planar embossing, is emerging as a viable fabrication technology which provides advantages such as reduced cycle time and large processing area. This includes roll-to-roll (R2R) thermal embossing and variants (Paul et al. 2007).

In this work, we describe a hot-roll-embossing process for manufacturing a flexible Y-microreactor in thin thermoplastic polymer foils of PMMA and COC using a microstructured silicon wafer as a flat embossing tool. We also investigated the sealing of the fluidic level with different techniques and tested the device to demonstrate mixing.

2 Materials and method

2.1 Films

Different thermoplastic materials were chosen as substrate for embossed microfluidic device: Topas 8007 cyclic olefin

copolymer (COC) from Ticona GmbH and Poly-methyl-methacrylate (PMMA) foils (Goodfellow) of respective nominal thickness of 130 and 125 μm . Their glass transition temperature (T_g) is equal to 78 and 105°C respectively.

Commercial SU8 Dry Film Resist from Microchem (XP MicroformTM-DF series) of 20 μm nominal thickness was also used for roll embossing trial and sealing. The epoxy foil is sandwiched between two protective layers, a bottom one of 60 μm thick mylar (polyester) and a top one of 30 μm thick polyethylene. The uncross-linked SU8 has a glass transition temperature (T_g) equal to 55°C.

2.2 Si-mould fabrication

A mask for a Y-microreactor pair was designed using Cadence software. The dimension of each microreactor is 4.6 cm \times 2.2 cm, and all microchannels are of 100 μm width. The optical mask was fabricated using a DWL200 laser pattern generator.

The mould was fabricated on a 1 mm thick 3" silicon wafer by means of photolithography and dry etching techniques. After the photolithographic step the wafer was dry etched in fluorine plasma by sequentially combining deep reactive ion etching (DRIE) and reactive ion etching to achieve positively tapered sidewalls to allow for easy demoulding. The first dry etching step in silicon was performed in an Adixen (Alcatel Vacuum Technology) A 601 E etcher using octo-fluoro-butane (C_4F_8) and sulphur hexafluoride (SF_6) gases.

After removal of the photoresist mask an RIE etching step was performed in SF_6 plasma in a Fluorine Plassys RIE etcher. Finally, an anti-sticking Teflon-like layer was then deposited on the etched wafer using an C_4F_8 plasma to facilitate further mould release.

2.3 Replication process

Hot embossing is a thermo-compressive process that takes place at a temperature just above the glass transition temperature of polymers. It exists in several configurations, planar or roller configuration and their variants. The roll embossing process is the case considered in this work and is illustrated in Fig. 1. It requires shorter time cycle than the planar process, as the polymer continuously advances (Sahli et al. 2009).

The equipment used for roll embossing of the fluidic level in COC and PMMA is a Rohm and Haas 350 HR laminator which consists of two rolls of metal covered with a rubbery material. These rolls can be heated and regulated independently of each other. The rotating motor is attached to the lower roller, the speed of rotation being an adjustable parameter. The upper roller has a degree of freedom in

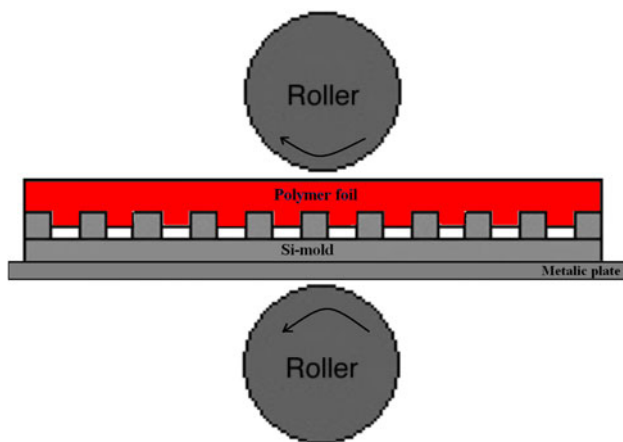


Fig. 1 Configuration of the roll embossing process used in this work

vertical translation allowing two positions, separation or contact (with the lower roller). The contact pressure is adjustable via a relief valve pressurized by air supply. The upper roller is rotated by transmission during contact with the lower roller. A temperature range from room temperature to 130°C is allowed for both rollers independently. The pressure can be adjusted from zero to eight bars and the feed rate can be increased continuously up to 3 m/min.

Experiments as a function of temperature of both rollers, applied pressure, feeding rate, and number of passes were conducted to optimize the filling of micro-cavities of the embossing tool. The microstructured Si-mould was placed on a supporting metallic plate of 1.5 mm, and the thermoplastic film was cut into parts that fit the structured Si area. The stamp-polymer assembly was then forced to pass between both embossing rollers under given embossing pressure, temperatures, and rolling speed.

The Process parameters were optimized by the classical one-dimensional search method involving the modification of one independent variable (such as the pressure, temperature, etc.) while fixing others at certain levels. Initial process parameters (temperatures of rollers) were selected according to the glass temperature [T_g] of the thermoplastic foil. The temperature of the upper roller which faces the polymer foil is set to a temperature lower than its T_g . On the other side the lower roller temperature facing the metallic plate that holds the Si-mould was set to a temperature much higher than the T_g . The temperature of both rollers was varied in the range of 50–130°C stepwise in steps of 10°C, the pressure in the range of 0.5–6 bar by step of 0.5 bar and feed rate up to 3 m/min.

The quality of the replica was assessed as a function of the replication depth, fair edge sharpness and release of the trapped air bubbles. Both mould and replicas were characterized using optical microscopy (Leica), profilometry (Tencor Alpha-Step 200) and scanning electron microscopy (SEM; Leica Cambridge Stereoscan S-440).

The profilometry measurements were done after observing under an optical microscope that there is no fault in the replica. The replica was then observed under the SEM to check the fidelity of the replica edges.

2.4 Sealing and interconnection

In this work two different sealing methods as well as two interconnection methods were investigated. The first sealing process was based on the lamination technique with SU8 DFR (Khan-Malek and Robert 2008). The same laminator as described above for the roll embossing process was used for lamination of SU8 foils as in Fig. 2. Optimization of the lamination parameters was performed by fixing all variables and changing only one to achieve a well sealed device with no air bubbles and clog-free channels.

The second sealing method investigated utilized a PDMS solution (Chow et al. 2006) that was spin-coated on the COC substrate. The spin coating was done in two stages, first a slow spinning with a speed of 300 rpm, acceleration of 400 rpm/sec for 10 s followed by fast spinning of 1,000 rpm, acceleration of 900 rpm/sec for 90 s to achieve a 30 μm PDMS layer (Koschwanetz et al. 2009). The PDMS was then cured in a furnace at 70°C for 2 h.

In order to achieve the interconnection of the microreactor chip with the syringe pump, a commercially available Nanoport connector assembly from UpChurch Scientific (N-333, WA, USA) composed of a threaded nut and ferrule system was used. Holes were punched through the film of COC covered with cured PDMS spin coated overall. Because of the relatively low glass transition temperature of Topas 8007 COC, these fittings were integrated onto chip reservoirs either directly by means of adhesive tape or using an intermediate printed circuit board (PCB) with epoxy glue. The PCB piece was glued directly to the Nanoport connector at 170°C for 1 h according to the Upchurch datasheet, and the PCB-nanoport assembly were then clamped to the fluidic level.

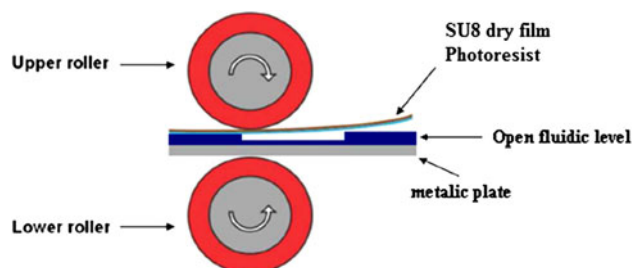


Fig. 2 Schematic for the lamination process

2.5 Test of the microreactor

In microfluidics, dyes are usually used to demonstrate the operation of the fluidic level. Changing the color of the solution was used here to show the mixing of the solutions in the microreactor used as a micromixer.

As illustrated, syringe pumps (Harvard Apparatus 11 series) were used with 5 ml syringe (Hamilton Gastight® 1005 RN) which has a plunger tip of poly-tetrafluoroethylene (PTFE), for use with gases and liquids. Connection of syringes to the Nanoport was performed using polyether-ether-ketone (PEEK) female Luers adaptor and fittings (Upchurch, P-659 and F-120 respectively). This system is suited to the channel section near 0.1 mm^2 , which avoids excessive loss of fluid.

Two different dye aqueous solutions with sodium lauryl sulfate (CAS 151-21-3 from Sigma) as surfactant, methyl Orange (CAS 547-58-0 from Sigma-Aldrich) and methyl Blue (CAS 28983-56-4 from Fluka), were introduced in the microreactor to observe the mixing under digital camera installed on the optical microscope. Varying the speed of a motor that pushes the plunger of a syringe connected to the channel through flexible tubes allows controlling the flow in the pump, shown in Fig. 3. The flow was set at $3 \mu\text{L}/\text{min}$ at both inlets, which is considered a relatively low flow value.

3 Results and discussion

3.1 Si-mould results

The sequential dry etching process was developed to obtain microstructures with tapered walls as shown in Fig. 4 to ease the demoulding of the polymer replica from the Si-

mould. The first DRIE step led to this sloped profile using a modified Bosch process with under-passivation by reducing the passivation flow gas and cycle time. This angle is close to 80° as the inset in Fig. 4 shows, meaning that the final upper width of the channel will be a factor of the etching depth. The following equation shows this relation:

$$W \cong W_0 - 2(d \times \tan 10^\circ), \quad (1)$$

where W denotes the final upper width, W_0 is the designed width and d is the etching depth. Applying Eq. (1) for $100 \mu\text{m}$ initial channel width and $30 \mu\text{m}$ depth the upper width will be approximately $90 \mu\text{m}$. One can also notice an undercut at the silicon top edge and also a somewhat rougher sidewall, which can be explained by the lower passivation time in the DRIE process. The following RIE step was used to suppress the Si undercut and the roughness of the pattern.

3.2 Replication results

Two main criteria were taken into consideration in order to define fidelity of replication, the feature profile on one hand and the transfer depth on the other hand. Two definitions will be used accordingly; “Adequate embossing” means satisfactory transferred depth and “fair replication” means acceptable replication in quality.

The Si ridges heights at different points at the whole wafer were measured using mechanical profilometry and it was found to vary between 30.7 and $31.22 \mu\text{m}$. Table 1 summarizes results obtained for the depth of replicas in COC and PMMA (d_{COC} , d_{PMMA}) under given processing conditions. Temperatures (Tupper, Tlower) were measured in $^\circ\text{C}$, pressure (P) in bars, feed rate (v) in m/min and number of passes (n).



Fig. 3 Set-up of the microreactor test

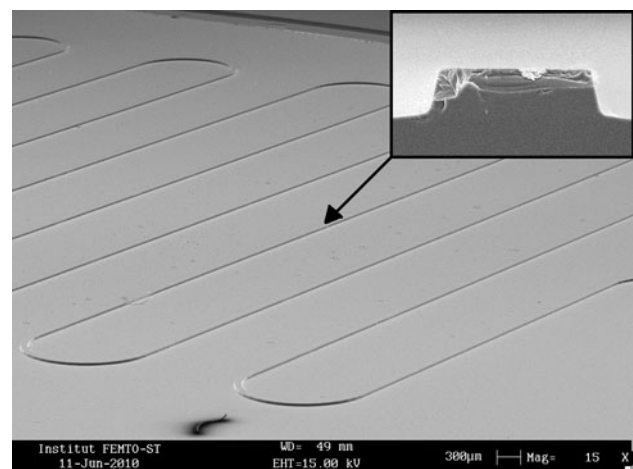


Fig. 4 SEM picture of dry-etched Si-stamp with microreactor pattern. *Inset*: profile of a silicon ridge cross-section

Table 1 Depth measurements at different process parameters

T_{upper}	T_{lower}	P	v	n	d_{COC}	d_{PMMA}	Remarks
50	50	4	0.5	1	1.95		
70	70	4	0.5	1	6		
80	80	4	0.5	1	7.4		
100	100	4	0.5	1	20.24	4.96	
110	110	4	0.5	1	30.77	9.79	COC transparency changes
120	120	4	0.5	1		14.24	COC tends to stick to roll at $T > 120^{\circ}\text{C}$
130	130	4	0.5	1		22.41	Max. temp. was reached but not enough
70	110	5.5	0.5	1	31.23		Fair replica with good transparency
130	130	5.5	0.1	1		30.38	
130	130	5.5	0.1	2		30.8	
130	130	5.5	0.1	3		30.97	
130	130	5.5	0.1	4		31.21	

3.2.1 Replication of Topas 8007

The replica with microchannels roll embossed in COC foil (Fig. 5) along with corresponding silicon mould with microridges of 100 μm width and 30 μm depth are illustrated in Fig. 4. It was produced in a single pass for the COC at a temperature of 70–110 $^{\circ}\text{C}$ for upper and lower rolls, respectively, using a pressure of 5.5 bar and a feed rate of 0.5 m/min.

In the COC replica, the smaller width of the ridge between two parallel microchannels is caused by the sloped channel sidewalls as observed in Fig. 6a, due to the smoothness of the polymer corners after mould release. This lack of sharp edge in the replica obtained with R2R method was attributed by Seo et al. (2007) to the absence of cooling stage in the R2R process (see Fig. 6b). On the other hand, Miserere group (Paul et al. 2007) proposed that the smoothness in the edge of the replica was a result of the low embossing temperature at the embossing surface as they used Ordyl dry film resist-based mould which dissipate relatively more heat compared to silicon which has a better thermal conductivity. They used an office laminator at the highest temperature 130 $^{\circ}\text{C}$, lowest speed 0.5 m/min and with minimum gap for the replication process in Topas 8007 COC foils. One year later the same group reported embossing trials at the higher temperature of 180 $^{\circ}\text{C}$ and obtained almost straight walls (Miserere et al. 2008). However, raising the embossing temperature increases the residual stress in the polymer (Yang et al. 2008). The polymer relaxation could be another explanation for

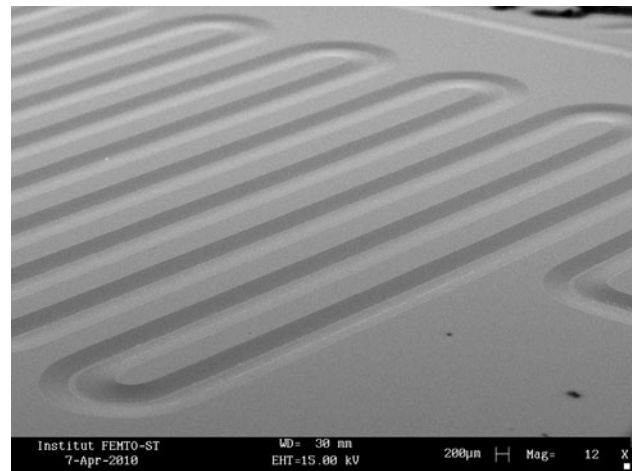


Fig. 5 SEM pictures for replicated COC from Si master by roll embossing

smoothing the edges of the embossed structures. The absence of cooling step coupled to the short holding pressure time could also contribute to this edge smoothness. The holding pressure forces the polymer to flow in the cavity and fill it. However, in roll embossing the pressure is only maintained for a short while which depends on the rolling speed. The cooling stage reduces the energy gained at the heating stage which is responsible for molecular motion in the polymer; upon cooling the polymer is let to keep the shape of the cavity of the mould.

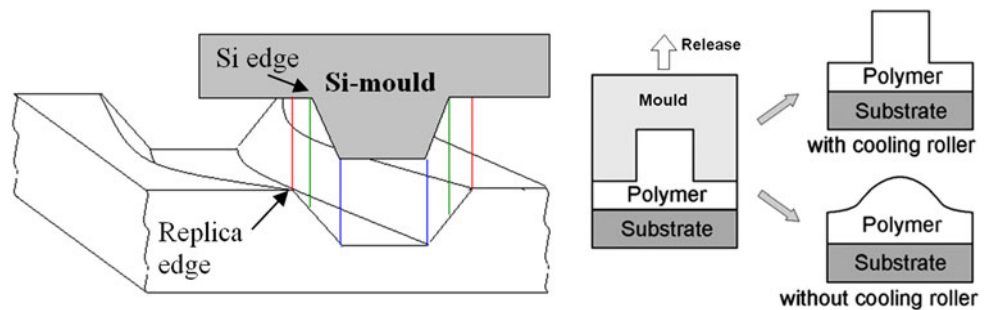
3.2.2 Replication of PMMA

The embossing of the PMMA foil in one single pass was not satisfactory even at the maximum laminator temperature of 130 $^{\circ}\text{C}$: the depth was not sufficient and the edges were not sharply defined. The number of passes was therefore taken in consideration as a solution for proper pattern transfer in the film. Each pass through the rollers not only pre-heated the PMMA foil for the next pass but also achieved deeper embossing in the polymer foil. For the microchannels in PMMA four passes were required at a temperature of 130 $^{\circ}\text{C}$ for both the upper and lower rollers while applying a pressure of 5.5 bar and a feed rate of 0.1 m/min (see Fig. 7). The number of passes improved the fidelity of replication concerning quality parameters such as embossed depth and edge smoothness. The edge smoothness was assessed by SEM observation. A smaller edge smoothness appears in PMMA compared to the one in COC. That is due to different processing parameters and material properties.

3.2.3 Replication of SU8

Limited results were obtained with SU8 foil which was found to stick to the microfeatures of the silicon stamp, even after it

Fig. 6 **a** Si-mould slice at a curve; **b** Schematic of embossing with and without cooling stage (Seo et al. 2007)



was covered with a conformal fluorinated layer. It is not the final statement for the SU8 replication because there are other groups who succeeded to hot emboss in SU8 using Si stamps, however only with step and repeat technique as it offers full control of the temperature cycle.

In order to study the reproducibility of the device, the uncertainty of the process was calculated through running experiments at fixed optimized parameters for five times according to ISO 15530-3. For each replica, transferred depth was measured five times; both mean and standard deviation of measurements were calculated in order to identify the uncertainty due to repeatability, the material thermal expansion, and also the uncertainty of the profilometry. Finally, measuring uncertainty was found to be less than 0.3 μm and the whole process uncertainty was 0.8 μm . Table 2 shows different measurements of the transferred depths of the five replicas with the standard deviation of the measurements and the calculated uncertainties.

3.3 Sealing and fluidic connections

The bonding of unexposed SU8 to SU8 was good after optimization of the lamination parameters to 65–75°C for upper and lower roller respectively, pressure of 2 bar and

speed of 1 m/min. The un-optimized parameters either face a problem of delamination as in Fig. 8a or lead to blocking of the channels.

The concave shape of the channel cover (with respect to the cover plane) as shown in Fig. 8b was explained by Abgrall et al. (2008) as due to the sudden expansion of the trapped gas inside the channels while the SU8 is still not solid. However, the relaxation of the polymer after processing could be another explanation. When a polymer foil partially in contact with a supporting structure (e.g. wall of channel) is heated, the polymer part in contact bonds with the structure and when cooled down remains bonded, whereas the part which is not in contact follows a relaxation process, which results in the concave shape observed here.

The bonding of the SU8 with PMMA was good as shown in Fig. 9a. However, opening of the inlet and outlet ports in the SU8 cover by a photolithography step resulted in alteration of the PMMA fluidic level: indeed, during the removal of the unexposed SU8 in the propylene-glycol-methyl-ether-acetate (PGMA) developer, the PMMA film loses its robustness and transparency, which are important issues for flexibility and optical analysis in ultra thin microfluidic devices. The DFR sealing method allows adequate transparency but the reversible sealing with PDMS shown in Fig. 9b is the most optically transparent.

Testing of the microreactors was performed with devices sealed with PDMS as it offers optical clarity and reversibility in sealing. The adhesive-based interconnections shown in Fig. 10a were tested using fluorescence microscopy but leakage could be observed near the ports due to the dissolution of the adhesive tape in ethanol. The epoxy-based interconnection passed the test successfully in both flat and bent configurations (Fig. 10b). The flat configuration was the only one used in the microscopy test to assure fixed focus distance.

The microreactor was tested as a micromixer. The fluids entering from both inlet ports start mixing at the connection junction. The mixing of the two fluids along the channel length resulted in a variation of colour as observed in Fig. 11.

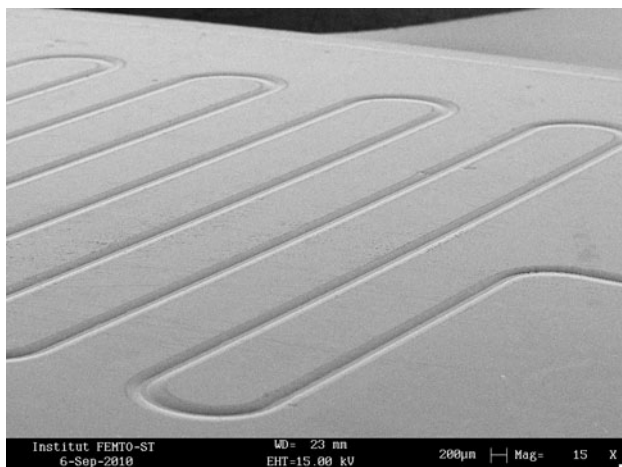


Fig. 7 SEM picture of channels with 100 μm width and 30 μm depth embossed in PMMA foil in four passes

Table 2 Measurements of the transferred depths of the five replicas and uncertainty of process

Replica	Measured value (μm)					Mean	Standard deviation	U_{0z} (μm)	u_{rep} (μm)	u_w (μm)	$U_{j,m}$ (μm)
	1	2	3	4	5						
No. 1	30.95	30.98	30.72	30.99	31.02	30.932	0.1211	0.0312	0.121	0.004	0.2
No. 2	30.83	30.94	31.09	30.8	30.9	30.912	0.1139	0.0312	0.114	0.004	0.2
No. 3	31.62	31.53	31.35	31.57	31.61	31.536	0.1099	0.0312	0.110	0.004	0.2
No. 4	31.66	31.91	31.66	31.64	31.81	31.736	0.1189	0.0312	0.119	0.004	0.2
No. 5	30.62	30.82	30.64	30.56	30.85	30.698	0.1289	0.0312	0.129	0.004	0.3
						31.163	0.4224	0.0312	0.422	0.004	0.8

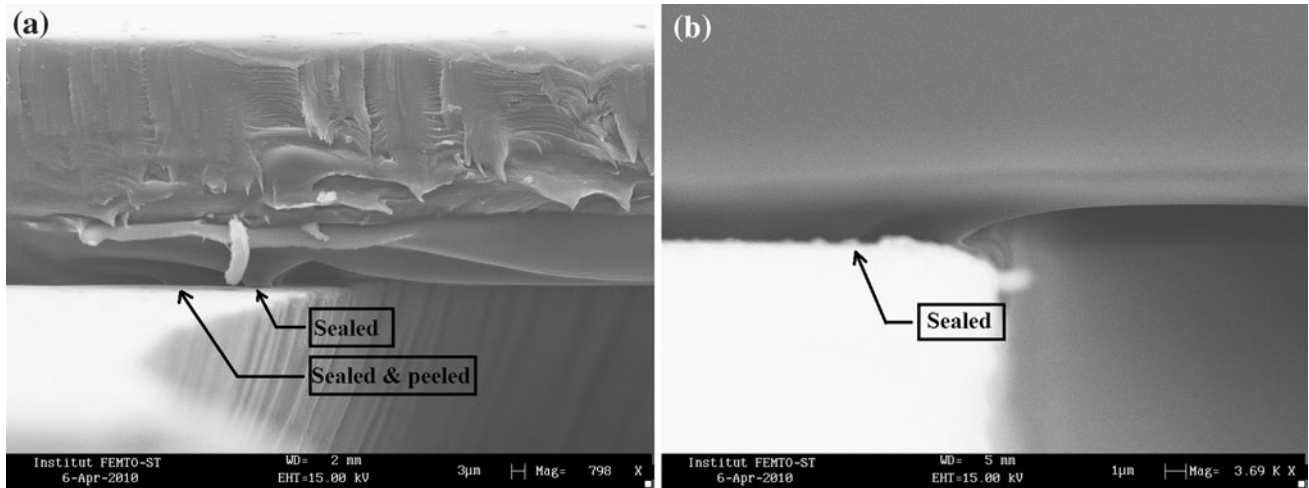


Fig. 8 SEM pictures of: **a** unexposed SU8 to SU8 bonding before optimization of parameters, **b** optimized parameters for unexposed SU8 to SU8 bonding

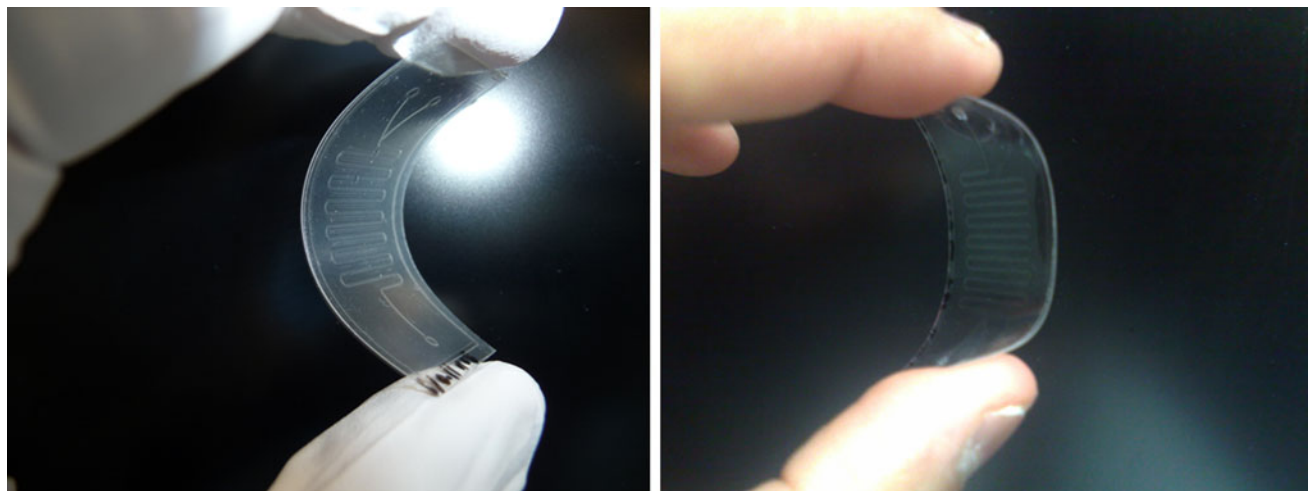


Fig. 9 Optical pictures of: **a** PMMA replica sealed with SU8 before definition of connection ports by photolithography; **b** COC replica sealed with COC-PDMS cover with punched ports

The disposability of devices is directly depending on cost. With the commercial semi-finished material used here and the large area processing allowed by the roll embossing process, a very low cost can be reached in

mass production. Breussin from Yole Development reported that disposable microfluidic devices will need production costs under 5 USD, for volumes ranging from 100,000 to 1 million units per year, in order to sell

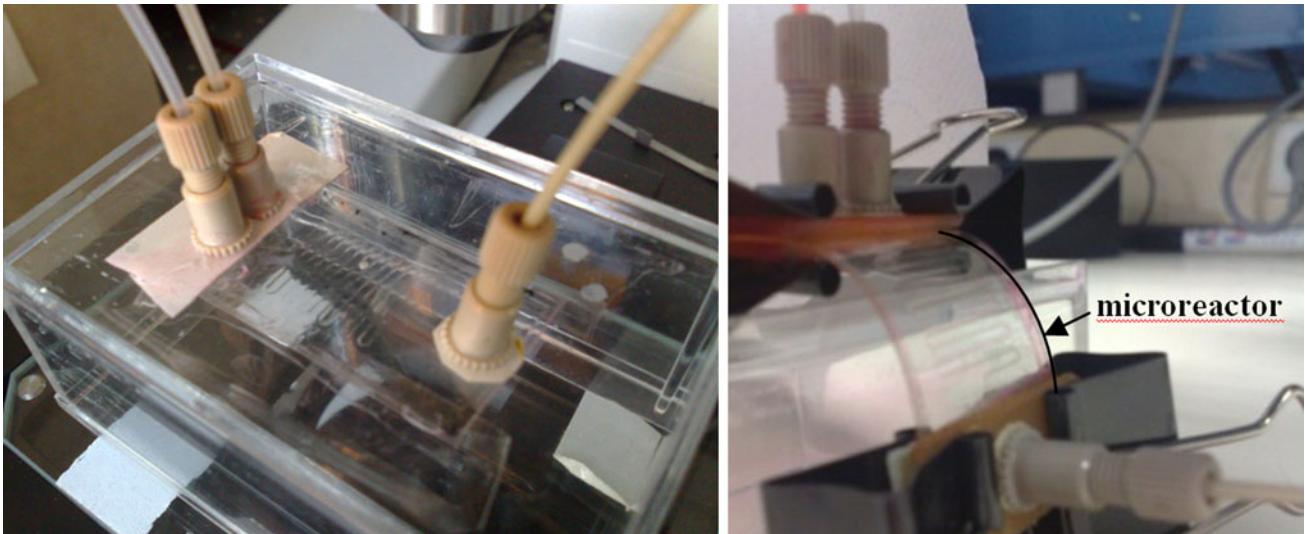


Fig. 10 Optical pictures of: **a** embossed microreactor with adhesive taped nanoport interconnection; **b** flexible microreactor in bent mode using epoxy-fixed nanoport interconnection

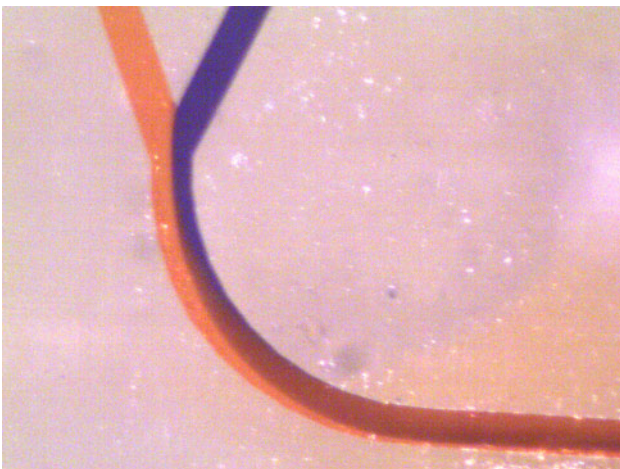


Fig. 11 Optical microscopy picture for diffusion zone of the two dye solutions in the microchannel

commercial tests for 50–100 USD including reagents (Breussin 2010).

4 Conclusion

A disposable flexible thin microreactor was fabricated by means of roll embossing, sealed and tested for liquid flow using optical microscopy. Microfeatures of 95 μm mean width and 30 μm depth were successfully replicated by roll embossing in one pass for Topas 8007 COC, and four passes for PMMA using a dry-etched flat Si mould. The temperatures of the rollers were selected and optimized to achieve adequate embossing depth and fair replication quality without increasing the residual stress in the finished

polymer. Limited results were obtained with SU8 foil which was found to stick to the microfeatures of the silicon stamp. Replicas in PMMA and Topas 8007 COC were sealed with SU8 cover by lamination. However, sealing of COC with SU8 was poor. A reversible PDMS sealing was therefore used with COC, which led to good sealing in both flat and bent configurations. Interconnection of the microreactor was done by means of commercial ports with adhesive tape and epoxy. The epoxy bonding was performed using an intermediate PCB to reach the bonding temperature and allow flexible configuration. The mixing of the two different dye solutions in the passive micromixer showed variation in colour along the microchannel length.

Acknowledgments This work was performed within the framework of Carnot-Fraunhofer French-German project “3 μP -Microfluidic platform for multiple samples with multiple analytics to run diagnostic analysis” and the SPIM doctoral programme from University of Franche-Comté.

References

- Abgrall P, Lattes C, Conédéra V, Dollat X, Colin S, Gué AM (2006) A novel fabrication method of flexible and monolithic 3D microfluidic structures using lamination of SU8 films. *J Micro-mech Microeng* 16:113–121
- Abgrall P, Charlot S, Fulcrand R, Paul L, Boukabache A, Gué AM (2008) Low-stress fabrication of 3D polymer free standing structures using lamination of photosensitive films. *J Microsyst Technol* 14:1205–1214
- Breussin F (2010) Infectious diseases will be best market for on-site diagnostics, but development will take some time still. *MEMS trends* 1:8–9
- Chow WW, Lei KF, Shi G, Li WJ, Huang Q (2006) Microfluidic channel fabrication by PDMS-interface bonding. *J Smart Mater Struct* 15:S112–S116

- Fiorini GS, Chiu DT (2005) Disposable microfluidic devices: fabrication, function and application. *BioTechniques* 38:429–446
- Focke M, Faltin B, Müller C, Zengerle R, Felix von Stetten (2009) Blow molding of microfluidic structures for Lab-on-Foil applications. Berlin Microsystem Technique Congress 12–14. Oktober 22
- Focke M, Kosse D, Müller C, Reinecke H, Zengerle R, von Stetten F (2010) Lab-on-a-foil: microfluidics on thin and flexible films. *Lab Chip* 10:1365–1386
- Garnier F, Hajlaoui R, Yassar A, Srivastava P (1994) All-polymer field-effect transistor realized by printing techniques. *Science* 265:1684–1686
- Khan-Malek C, Robert L (2008) Flexible microfluidics based on commercial SU8 foils. In: Dimov S, Menz W (eds) Proceedings of the 4th Int. Conference Multi-Material Micro Manufacture (4M2008), Cardiff, UK, 9–11 Sept, pp 96–99
- Khan-Malek C, Robert L, Salut R (2009) Femtosecond laser machining and lamination for large-area flexible organic microfluidic chips. *Eur Appl Phys* 46(1):12503–12508
- Koschwanetz JH, Carlson RH, Meldrum DR (2009) Thin PDMS films using long spin times or *tert*-butyl alcohol as a solvent. *PLoS one* 4(2):e4572–e4577
- Miserere S, Weber J, De Lambert B, Viovy JL, Malaquin L (2008) A toolbox for lamination—based fast prototyping of flexible monolithic COC chips. In: Proceedings of the 1st European conference on Microfluidics, Microfluidics-2008, Bologna, 10–12 Dec 2008
- Nambiar AN (2009) A supply chain perspective of RFID systems. *World Acad Sci Eng Technol* 60:877–881
- Nunes PS, Ohlsson PD, Ordeig O, Kutter JP (2010) Cyclic olefin polymers: emerging materials for lab-on-a-chip applications. *Microfluid Nanofluid* 9:145–161
- Nystrom G, Razaq A, Strømme M, Nyholm L, Mihranyan A (2009) Ultrafast all-polymer paper-based batteries. *Nano Lett* 9:3635–3639
- Paul D, Pallandre A, Miserere S, Weber J, Viovy JL (2007) Lamination-based rapid prototyping of microfluidic devices using flexible thermoplastic substrates. *J Electrophor* 28(7):1115–1122
- Sahli M, Khan-Malek C, Gelin JC (2009) 3D modelling and simulation of the filling of cavities by viscoelastic polymer in roll embossing process. *Int J Mater Form* 2(1):725–728
- Sarma KR, Roush J, Schmidt J, Chanley C, Dodd S (2006) Flexible active matrix organic light emitting diode displays. In: Proceedings of ASID'06, New Delhi, 8–12 Oct 2006, pp 337–342
- Seo S, Kim T, Lee HH (2007) Simple fabrication of nanostructure by continuous rigiflex imprinting. *J Microelectron Eng* 84:567–572
- Tsai YC, Yang SJ, Lee HT, Jen HP, Hsieh YZ (2006) Fabrication of a flexible and disposable microreactor using a dry film photoresist. *J Chin Chem Soc* 53:683–688
- Velten T, Schuck H, Richter M, Klink G, Bock K, Khan-Malek C, Roth S, Schoo H, Bolt PJ (2008) Microfluidics on foil: state of the art and new developments. *J Eng Manuf Part B* 222(1):107–116
- Wohrle D, Meissner D (1991) Organic solar cells. *Adv Mater* 3:129–138
- Yang SY, Huang TC, Ciou JK, Chan BD, Loeser JG (2008) CO₂-assisted embossing for the fabrication of PMMA components under low temperature and with low pressure. *J Micromech Microeng* 18:25024–25031